Immobilized Small Deoxyribozyme to Distinguish RNA Secondary Structures†

Yasuhide Okumoto,‡ Tatsuo Ohmichi,§ and Naoki Sugimoto*,‡,§

Department of Chemistry, Faculty of Science and Engineering and High Technology Research Center, Konan University, 8-9-1 Okamoto, Higashinada-ku, Kobe 658-8501, Japan

Received October 10, 2001; Revised Manuscript Received December 7, 2001

ABSTRACT: The RNA folding variation due to one or more mutations leads to different RNA splicing, RNA processing, and translational controls as a result of differences in the primary and higher-ordered structures that interact with other cellular molecules. Thus, distinguishing RNA folding is one of the guides to detect the gene functions related to disease and drug responses. We found, previously, a small Ca^{2+}-dependent deoxyribozyme with its site-specific RNA cleavage [Sugimoto, N., Okumoto, Y., and Ohmichi, T. (1999) *J. Chem. Soc., Perkin Trans. 2*, 1382−1388]. In this study, we report the potential of this deoxyribozyme as a useful tool to distinguish RNA foldings. It is found that the immobilized deoxyribozyme using avidin−biotin interaction cleaves the target site within only single-stranded RNAs. The systematic design for the target RNA hairpin loops shows that the immobilized deoxyribozyme is able to cleave them with a ≥17 nucleotide loop size at only one site under single-turnover conditions. Furthermore, an RNA cleavage reaction is detected using the immobilized deoxyribozyme on a surface plasmon resonance (SPR) sensor chip. These results show that the immobilized deoxyribozymes on a column and on an SPR sensor chip become a novel and useful tool to distinguish the RNA foldings.

Oligonucleotide captures for sequence-specific analysis have been developed as new biotechnologies of DNA chips and microarrays (*1*). These biotechnologies are very powerful tools for the genomic analysis of SNPs[1] and mRNA/gene expressions (*2*, *3*). However, it is difficult using these methods to detect the difference in RNA folding. The RNA folding variation due to one or more mutations would lead to different biological functions as a result of differences in the primary or higher-ordered structures that interact with other cellular molecules, because the RNA folding influences the RNA splicing, processing, and so forth (*4*, *5*). Thus, to distinguish the RNA foldings is one of the guides to detect the gene functions related to diseases and drug responses.

Ribozymes and deoxyribozymes (catalytic nucleic acids) are catalysts in biochemical reactions and of interest for pharmaceutical application (*6*−*15*). Recent studies on deoxyribozymes showed specifically that they are also interesting tools in biotechnology because they are simple, stable, and cost-effective. For a cleavage reaction using a catalytic nucleic acid, the cleavage activity is basically dependent on the sequence close to the cleavage site. Furthermore, the RNA cleavage efficiency by the catalytic nucleic acid is actually dependent on the secondary structure of the target RNA, because the stem regions within the cleavage site have the potential to lock the binding of the catalytic nucleic acid to the target sites. This fact indicates the possibility for the catalytic nucleic acid to distinguish or detect the target RNA foldings. However, although all catalytic nucleic acids have the potential to distinguish the structure of the nucleic acids as novel application tools, the effect of the RNA folding on the cleavage efficiency has apparently not been investigated.

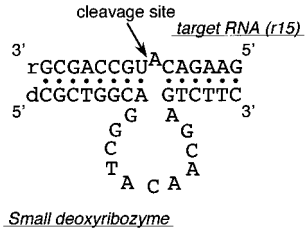

FIGURE 1: Secondary structure of the complex of the small Ca^{2+}-dependent deoxyribozyme and its target RNA substrate (r15). The deoxyribozyme binds its target through two substrate-recognition domains, each involving Watson−Crick base pairs (closed circles).

We made previously a small Ca^{2+}-dependent deoxyribozyme by downsizing the 10−23 deoxyribozyme, derived from the 23rd round clone obtained after the 10th round of the in vitro selection procedure by Joyce et al., from the viewpoint of rational design as shown in Figure 1 (*16*, *17*). The catalytic efficiency of the small deoxyribozyme in the presence of Ca^{2+} was, interestingly, about 24-fold larger than those of Mg^{2+} indicating that the small deoxyribozyme has a higher metal ion selectivity than the 10−23 deoxyribozyme. Here, we have now developed an immobilized small deoxy-

† This work was supported in part by Grants-in-Aid for Scientific Research from the Ministry of Education, Science, Sports and Culture, Japan, and a Grant from "Research for the Future" Program of the Japan Society for the Promotion of Science.

* To whom correspondence should be addressed: Naoki Sugimoto, Professor of Chemistry and Director of High Technology Research Center. Phone: +81-78-435-2497. Fax: +81-78-435-2539. E-mail: sugimoto@konan-u.ac.jp.

‡ Department of Chemistry, Faculty of Science and Engineering.

§ High Technology Research Center.

[1] Abbreviations: SNPs, single nucleotide polymorphisms; nt, nucleotides; HPLC, high-performance liquid chromatography; dU, 2′-deoxyuridine; ATPγS, adenosine-5′-O-(3-thiotriphosphate); 5-IAF, 5-iodoacetamidofluorescein; Tris, tris(hydroxymethyl)aminomethane; EDTA, ethylenediaminetetraacetic acid; k_{obs}, observed rate constant; SPR, surface plasmon resonance; RU, resonance units; T_m, melting temperature.

10.1021/bi011909c CCC: $22.00
Published on Web 02/01/2002

ribozyme as a novel and useful tool to distinguish RNA foldings. As a result, the immobilized deoxyribozyme was able to cleave the RNA hairpin with a ≥17 nt loop size at only one site. Furthermore, an RNA cleavage reaction is detected using the immobilized deoxyribozyme on an SPR sensor chip. Thus, the immobilized deoxyribozyme was able to distinguish the higher-ordered structures of nucleic acids.

MATERIALS AND METHODS

Materials. The DNA and RNA oligomers were synthesized chemically and purified by reversed-phase HPLC and electrophoresis on 20% polyacrylamide/7 M urea denaturing gel, as described previously (*16*, *17*). The biotin and dU phosphoramidites were purchased from Glen Research Co., Ltd. (Sterling, VA). The final purity of the oligonucleotides was confirmed to be >99%. The oligonucleotides were desalted with a Sep-Pak C18 cartridge before use. Single-strand concentrations of the purified oligonucleotides were determined by measuring the absorbance at 260 or 280 nm. The single-strand extinction coefficients were calculated via mononucleotide and dinucleotide (*18*). The target was 5′-end labeled with ATPγS, T4 polynucleotide kinase and 5-IAF at 37 °C. The 5′-end biotinylated deoxyribozyme was immobilized on immunoPure avidin gel (Pierce, Rockford, IL) in a buffer containing 20 mM Na_2HPO_4 (pH 7.5) and 500 mM NaCl for a 20-min incubation at 25 °C.

Target Cleavage Reactions by the Deoxyribozyme. The methods of target cleavage reactions by the deoxyribozymes were done in a buffer containing 50 mM Tris-HCl (pH 8.0) and 25 mM Ca^{2+} under multiple-turnover conditions with 300 nM target and 15 nM deoxyribozyme or single-turnover conditions with 10 nM target and 200 nM deoxyribozyme at 37 °C (*16*, *17*). Removing aliquots from the reaction mixture at appropriate intervals and mixing them with 100 mM Na_2EDTA and 7 M urea terminated the cleavage reactions. The 5′-end fluorescein-labeled products and targets were separated by electrophoresis on 20% or 16% polyacrylamide/7 M urea denaturing gels. The target cleavage yields were determined by quantifying the fluorescence intensity in the bands of the 5′-end labeled products and targets using a Fluor-S MultiImager (Bio-Rad, Randolph, MA). The observed rate constants (k_{obs}) were calculated using the following equation (*19*):

$$[P] = [P]_\infty(1 - e^{-k_{obs}t}) \quad (1)$$

where [P] is the cleavage yield, $[P]_\infty$ is the final cleavage yield, and t is the reaction time. Nonlinear least-squares fits in the plots of the cleavage yield versus reaction time to the kinetic equation were done with Igor ver1.27 software (Wave Metrics, Inc.) to obtain the k_{obs} values.

Target Cleavage Reactions using the Deoxyribozyme Array. A BIAcore (BIAcore 1000, Biacore AB, Uppsala, Sweden) was used for the SPR measurements (*17*). The SPR signal is expressed in relative RU (resonance units) plotted against time in a sensorgram (see Figure 4). The 1 of the relative RU is approximately equivalent to a change in surface concentration of about 0.15 ng/mm^2 for most biomolecules (*20*). The 5′-end biotinylated deoxyribozyme was immobilized to the bound streptavidin on the SPR sensor chip to give about 4 relative RU. To remove the background binding between the injected target and the immobilized streptavidin to the dextran matrix or the refractive index change in the injection, the SPR trace, after flowing a buffer containing the target over the sensor chip coated without the ligand, was deducted from those with the ligand. The target was injected in a buffer containing 50 mM Tris-HCl (pH 8.0) and 100 mM Na^+ at 37 °C at the slow flow rate of 5 μL min^{-1}. The concentration of the injected target was 100 μM. By addition to 25 mM Ca^{2+}, the target cleavage reactions were initiated.

RESULTS AND DISCUSSION

Immobilized Deoxyribozyme Detects the Difference in the RNA Foldings. The immobilized deoxyribozyme as a useful tool to investigate the RNA foldings is better than the free deoxyribozyme, because the immobilized deoxyribozyme has some advantages such as the easy separation between the deoxyribozyme and the cleavage products and its ability repeated by use to be. Furthermore, in the immobilized deoxyribozyme as well as the free one, there is no burst kinetics during the early stage of the reaction (see Figure S1 in Supporting Information). The result suggests that the immobilized deoxyribozyme as well as the free one cleaves its target.

To obtain information about the effect of target foldings, we first investigated whether the immobilized deoxyribozyme cleaves the site within the duplex. We found that the immobilized deoxyribozyme was able to cleave the site only in the single-stranded RNAs, although the single-stranded DNA, RNA/DNA hybrid, and RNA/RNA duplex were not cleaved (see Figure S2 in Supporting Information).

The deoxyribozyme can recognize various targets by changing the sequences of its recognized domain. The catalytic activity depends on the thermodynamic stability of the stem domains in the catalytic nucleic acids and its substrate (*21*). For the hammerhead ribozyme, the free energy of the substrate binding by the ribozyme correlated well with the values estimated from the formation of the two substrate binding arms calculated using the nearest-neighbor parameters (*22*). The optimum stability of the stems in the complex was investigated. The prepared target RNAs have various lengths (see Figure S3a in Supporting Information). The stabilities of the stems within the complex of the immobilized deoxyribozyme and its RNA substrate were predicted using our nearest-neighbor parameters of the RNA/DNA hybrids (*23*, *24*). The predicted stability [predicted $\Delta G^\circ_{37(1M\ Na^+,stems)}$] was calculated from the following equation:

$$\text{predicted } \Delta G^\circ_{37(1\ M\ Na^+,stems)} = \Delta G^\circ_{37(left\ stem)} + \Delta G^\circ_{37(right\ stem)} \quad (2)$$

where $\Delta G^\circ_{37(left\ stem)}$ and $\Delta G^\circ_{37(right\ stem)}$ are the predicted values of the left and right stems, respectively. The result shows that the optimum reaction rates can be obtained within the range of stability from −10 to −20 kcal mol^{-1} and that the plot is symmetric (see Figure S3b in Supporting Information). When sensitivity is ≤20 kcal mol^{-1}, because the targets (r24, r22, and r20) are long RNA sequences, they have the possibility to form intramolecular structures of the RNAs. When sensitivity is ≥10 kcal mol^{-1}, because of the low

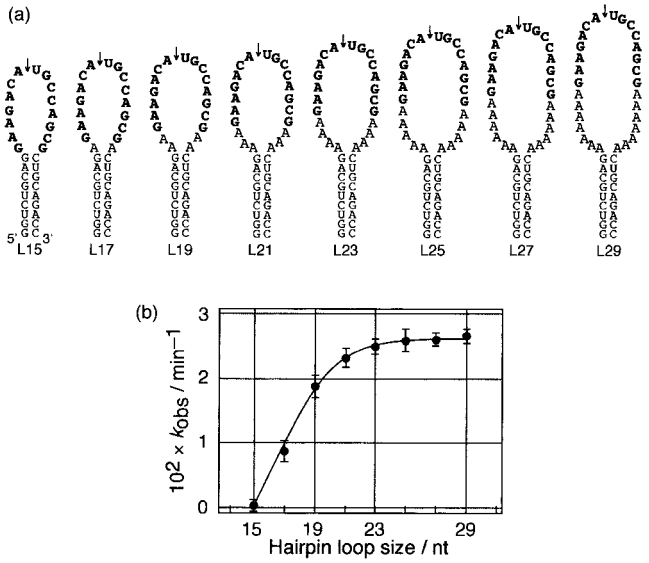

FIGURE 2: (a) Secondary structures of the complex of the RNA hairpin loops (L15, L17, L19, L21, L23, L25, L27, and L29). The arrow indicates each cleavage site. Boldface letters indicate domains recognized by the deoxyribozyme. (b) Plot of k_{obs} versus hairpin loop size. All experiments were done in a buffer containing 50 mM Tris-HCl (pH 8.0) and 25 mM Ca^{2+} at 37 °C.

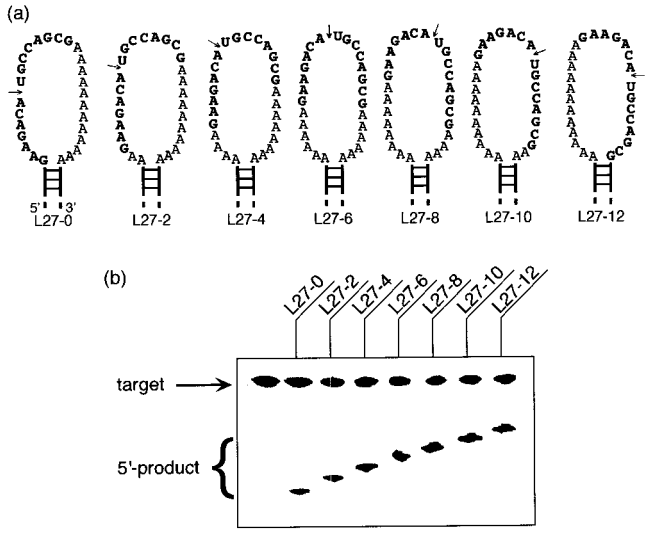

FIGURE 3: (a) Secondary structures of the complex of the RNA hairpin loops (L27−0, L27−2, L27−4, L27−6, L27−8, L27−10, and L27−12). The arrow indicates each cleavage site. Boldface letters indicate recognized domains by the deoxyribozyme. (b) Denaturing 16% polyacrylamide/7 M urea gel showing the cleavages of the target molecules by the immobilized deoxyribozyme in a buffer containing 50 mM Tris-HCl (pH 8.0) and 25 mM Ca^{2+} at 37 °C after a 60 min incubation.

stability in the right and left stems, it is difficult to form a complex of the deoxyribozyme and its target RNA substrate; then, the immobilized deoxyribozyme has low activity.

The single-stranded RNA regions are basically unpaired, such as in the hairpin loops and internal loops within the RNA foldings. To investigate the effect of the RNA hairpin loop size, the cleavage reactions of eight RNA hairpin loops by the immobilized deoxyribozyme were carried out in the presence of 25 mM Ca^{2+} (pH 8.0) under single-turnover conditions (see Figure 2a). The sequence of the hairpin loop of L15 is identical to that of r15. The main parts of the hairpin loop of L17, L19, L21, L23, L25, L27, and L29 are also identical to those in r15, and the 1−7 spacers (rAs) are also systematically added to both the 5′ and 3′ ends of these hairpin loops, respectively. These RNA sequences melted with biphasic behavior, and the T_m values were independent of the concentration of the RNAs (see also Figure S4 in Supporting Information), indicating that the folded structure of these RNAs would be the only stable intramolecular hairpin loop but not an intermolecular loop structure (*25*, *26*). The cleavage reactions of these various RNA hairpin loops by the immobilized deoxyribozyme were carried out. Figure 2b shows the relationship between the catalytic activity and the hairpin loop size. For L15, the cleavage reaction was little observed. On the other hand, for ≥17 nt as a hairpin loop size (L17, L19, L21, L23, L25, L27, and L29), the cleavage reactions were observed at only one site. These results suggest that at least one nucleotide spacer at both ends of the hairpin loop are required for efficient cleavage by the immobilized deoxyribozyme. The catalytic activity was saturated over ≥23 nt as the hairpin loop size (L23, L25, L27, and L29).

The cleavage position of the immobilized deoxyribozyme is important for detecting the difference in the RNA foldings. To investigate the effect of the cleavage position, the RNA hairpin loop cleavage reactions by the immobilized deoxyribozyme were carried out in the presence of 25 mM Ca^{2+} (pH 8.0) under single-turnover conditions. These hairpin loop sequences correspond to r15 and have 12 nt spacers (dAs), and the total hairpin loop sizes are the same as the 27 nt shown in Figure 3a. The RNA hairpin loop domain was systematically slid from the 5′ end to the 3′ end in the recognition site of the immobilized deoxyribozyme. These sequences melted with biphasic behavior, and the T_m was independent of the concentration of the RNAs (data not shown), showing that the folded structure would be a stable hairpin loop but not an internal loop structure. These RNA cleavage yields by the immobilized deoxyribozyme were approximately equal amounts, as shown in Figure 3b. This result indicates that any target position in the RNA hairpin loop is cleaved only at one site.

Development of the Deoxyribozyme Array on an SPR Sensor Chip. The construction and application of the immobilized deoxyribozyme on an SPR sensor chip to create a deoxyribozyme array has not been described. In this paper, we have already demonstrated that the novel and useful application tool of the deoxyribozyme array is possible, which may enable the rapid invention of numerous DNA biosensor elements with satisfactory performance characteristics. The same method should apply to the use of DNA and many nucleic acids analogues that can provide greater versatility for analysis recognition and increased stability in harsh environments. In this regard, the catalytic nucleic acid arrays could have long storage lives, perhaps greater than biosensor components made from natural protein. The RNA cleavage by the immobilized deoxyribozyme requires the binding and cleavage steps between the target RNA substrate and the immobilized deoxyribozyme. To clarify the properties of these steps, these processes were directly measured by an SPR apparatus in a buffer containing 50 mM Tris-HCl (pH 8.0) at 37 °C. Figure 4 shows the typical SPR sensorgrams of the binding and cleavage steps between the target RNA substrates (r15 and pseudo RNA substrate [rGAAGAC(dA)UGCCAGCG]) and the immobilized deoxy-

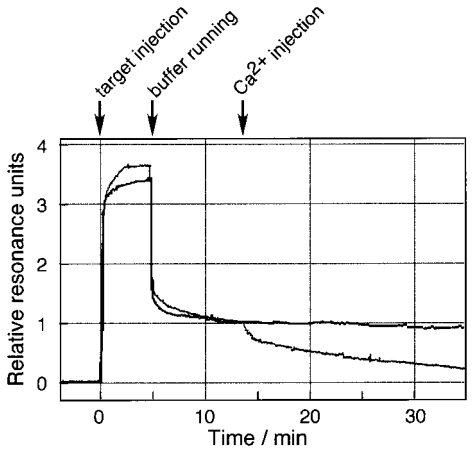

FIGURE 4: The typical SPR sensorgrams of the binding and cleavage steps between the target molecule and the immobilized deoxyribozyme on the SPR sensor chip in a buffer containing 50 mM Tris HCl (pH 8.0) at 37 °C. The flow samples were r15 (black line) or the pseudo RNA substrate (gray line).

ribozyme on the SPR sensor chip. When its target binds to the immobilized deoxyribozyme on the SPR sensor chip, the observed response unit is increased by changes in the refractive index as shown by the RU values in real time (*27*). When the pseudo RNA substrate was flowed over the sensor chip coated with the immobilized deoxyribozyme, about 1 of the relative RU value was retained by the addition to Ca^{2+}. However, in the case of r15, the relative RU value was slowly decreased by the addition to Ca^{2+}. The differences in the relative RU value after 30 min running was 69%. After the recovery of these samples, the cleavage products and targets were able to be separated by electrophoresis on 20% polyacrylamide/7 M urea denaturing gel (data not shown). As a result, no cleavage band was observed for the pseudo RNA substrate, while only one cleavage band was observed for r15. The cleavage site was at only one site of rAp↓U in the asymmetric internal loop. These results indicate that the decrease in the RU value shows the process of the product release after the RNA cleavage reaction.

Conclusion. In this study, we developed a novel and useful column and SPR sensor chip with an immobilized small Ca^{2+}-dependent deoxyribozyme. The optimum stability of the stems in the complex of the deoxyribozyme and its target RNA substrate should be within the range from −10 to −20 kcal mol^{-1}. The targets of the immobilized deoxyribozyme were most suitable for only single-stranded RNAs containing a hairpin loop with ≥17 nt loop size, neither for the single-stranded DNA, RNA/RNA, nor RNA/DNA hybrids. Thus, the immobilized deoxyribozyme can distinguish the higher-ordered structures of RNAs.

On the basis of our results, we propose a search system for RNA higher-ordered structures using the column and SPR sensor chip with the immobilized deoxyribozyme. We will then be able to construct a database of higher-ordered structures of genome and other nucleic acids. First, secondary structures of the sequences are predicted using nearest-neighbor parameters (*23*, *24*). Second, the analysis of the higher-ordered structures of RNAs is determined using the immobilized deoxyribozyme. Third, a comparison is made between the secondary structure predictions and the experimental results. If both agree, one tries to construct a database of the higher-ordered structure of the structural and functional genomes and the other nucleic acids. If both do not agree, one tries to add this information to the thermodynamic parameters of bulge, internal loop, mismatch, and so forth (*25*, *26*, *28*−*33*). Finally, we will be able to get an exact and useful database with this procedure.

SUPPORTING INFORMATION AVAILABLE

Figure S1 shows secondary structures of the complex of the immobilized deoxyribozyme and its target RNA, the relationship between the k_{obs} value and the stability ($\Delta G°_{37}$) of the stem regions in the immobilized deoxyribozyme−RNA substrate complex. Figure S2 shows the plots of the cleavage yield versus reaction time under multiple-turnover conditions. Figure S3 shows target sequences and denaturing 20% polyacrylamide/7 M urea gel showing the cleavages of the targets by the free or immobilized deoxyribozyme in the presence of 25 mM Ca^{2+} (pH 8.0) at 37 °C after a 20 min incubation. Figure S4 shows the normalized melting curves of RNA hairpin loops in a buffer containing 50 mM Tris-HCl (pH 8.0) containing 25 mM Ca^{2+}. This material is available free of charge via the Internet at http://pubs.acs.org.

REFERENCES

1. Debouck, C., and Goodfellow, P. N. (1999) *Nat. Genet. 21*, 48−50.
2. Selinger, D. W., Cheung, K. J., Mei, R., Johansson, E. M., Richmond, C. S., Blattner, F. R., Lockhart, D. J., and Church, G. M. (2000) *Nat. Biotechnol. 18*, 1262−1268.
3. Gentalen, E., and Chee, M. (1999) *Nucleic Acids Res. 27*, 1485−1491.
4. Mohan, A., and Levinger, L. (2000) *J. Mol. Biol. 303*, 605−616.
5. Barrette, I., Poisson, G., Gendron, P., and Major, F. (2001) *Nucleic Acids Res. 29*, 753−758.
6. Santoro, S. W., and Joyce, G. F. (1997) *Proc. Natl. Acad. Sci. U.S.A. 94*, 4262−4266.
7. Santoro, S. W., and Joyce, G. F. (1998) *Biochemistry 37*, 13330−13342.
8. Nakano, S., Chadalavada, D. M., and Bevilacqua, P. C. (2000) *Science 287*, 1493−1497.
9. McKay, D. B., and Wedekind, J. E. (1999) in *The RNA World* (Gesteland, R. F., Cech, T. R., and Atokins, J. F., Eds.) 2nd ed., pp 265−286, Cold Spring Harbor Laboratory Press, Plainview, NY.
10. Disney, M. D., Testa, S. M., and Turner, D. H. (2000) *Biochemistry 39*, 6991−7000.
11. O'Rear, J L., Wang, S., Feig, A. L., Beigelman, L., Uhlenbeck, O. C., and Herschlag, D. (2001) *RNA 7*, 537−545.
12. Marshall, K. A., and Ellington, A. D. (1999) *Nat. Struct. Biol. 6*, 992−994.
13. Seetharaman, S., Zivarts, M., Sudarsan, N., and Breaker, R. R. (2001) *Nat. Biotechnol. 19*, 336−341.
14. Hausch, F., and Jaschke, A. (2000) *Nucleic Acids Res. 28*, E35.
15. Li, J., and Lu, Y. (2000) *J. Am. Chem. Soc. 122*, 10466−10467.
16. Sugimoto, N., Okumoto, Y., and Ohmichi, T. (1999) *J. Chem. Soc., Perkin Trans. 2*, 1382−1388.
17. Okumoto, Y., and Sugimoto, N. (2000) *J. Inorg. Biochem. 82*, 189−195.
18. Richards, E. G. (1975) in *Handbook of Biochemistry and Molecular Biology: Nucleic Acids* (Fasman, G. D., Ed.) Vol. 1, pp 597, CRC Press, Cleveland, OH.
19. Sugimoto, N., Kierzek, R., and Turner, D. H. (1988) *Biochemistry 27*, 6384−6392.
20. (reprinted 1998) *BIAtechnology Handbook*, Version AB, Contents 2, Biacore AB, Uppsala, Sweden.
21. Ota, N., Warashina, M., Hirano, K., Hatanaka, K., and Taira, K. (1998) *Nucleic Acids Res. 26*, 3385−3391.

22. Hertel, K. J., Stage-Zimmermann, T. K., Ammons, G., and Uhlenbeck, O. C. (1998) *Biochemistry 37*, 16983−16988.
23. Sugimoto, N., Nakano, S., Katoh, M., Nakamuta, H., Ohmichi, T., Yoneyama, M., and Sasaki, M. (1995) *Biochemistry 34*, 11211−11216.
24. Turner, D. H., Sugimoto, N., and Freier, S. M. (1988) *Annu. Rev. Biophys. Biophys. Chem. 17*, 167−192.
25. Dale, T., Smith, R., and Serra, M. J. (2000) *RNA 6*, 608−615.
26. Kawakami, J., Yoneyama, M., Miyoshi, D., and Sugimoto, N. (2001) *Chem. Lett*. 258−259.
27. Karlin, S., and Broccheieri, L. (1996) *J. Bacterol. 178*, 1881−1895.
28. Zhu, J., and Wartell, R. M. (1999) *Biochemistry 38*, 15986−15993.
29. Burkard, M. E., Kierzek, R., and Turner, D. H. (1999) *J. Mol. Biol. 290*, 967−982.
30. Sugimoto, N., Nakano, M., and Nakano, S. (2000) *Biochemistry 39*, 11270−11281.
31. Wu, P., and Sugimoto, N. (2000) *Nucleic Acids Res. 28*, 4762−4768.
32. Schroeder, S. J., and Turner, D. H. (2000) *Biochemistry 39*, 9257−9274.
33. Dale, T., Smith, R., and Serra, M. J. (2000) *RNA 6*, 608−615.

BI011909C